

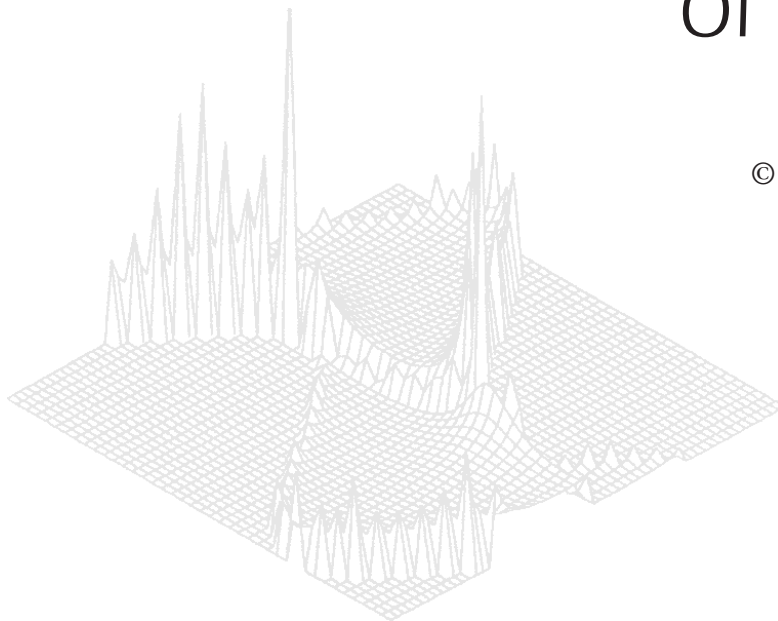
---

**C S I R O   P U B L I S H I N G**

---

# Australian Journal of Physics

Volume 50, 1997  
© CSIRO Australia 1997



A journal for the publication of  
original research in all branches of physics

**[www.publish.csiro.au/journals/ajp](http://www.publish.csiro.au/journals/ajp)**

All enquiries and manuscripts should be directed to

*Australian Journal of Physics*

**CSIRO PUBLISHING**

PO Box 1139 (150 Oxford St)

Collingwood

Vic. 3066

Australia

Telephone: 61 3 9662 7626

Facsimile: 61 3 9662 7611

Email: [peter.robertson@publish.csiro.au](mailto:peter.robertson@publish.csiro.au)



Published by **CSIRO PUBLISHING**  
for CSIRO Australia and  
the Australian Academy of Science



## Use of Transport Coefficients to Calculate Properties of Electrode Sheaths of Electric Arcs\*

*J. J. Lowke and J. C. Quartel*

Division of Applied Physics, CSIRO,  
PO Box 218, Lindfield, NSW 2070, Australia.

### *Abstract*

Particle conservation equations for electrons and positive ions, together with Poisson's equation to account for space-charge effects on the electric field, have been solved for the electrode sheath regions of electric arcs. For thermionic cathodes and the anode, we find that the ambipolar diffusion approximation is generally valid. At the surface of the anode we find that there is generally a small retarding electric field. For non-thermionic cathodes and no ionisation due to the electric field in the sheath, we calculate unrealistically high sheath voltages and even then, find that the electric fields at the cathode surface are insufficient for field emission. It is suggested that photoionisation in the region close to the cathode may be a principal source of electrons for non-thermionic cathodes.

### **1. Introduction**

Although arc columns are reasonably well represented as plasmas which are in local thermodynamic equilibrium, uncertainties exist as to the importance of basic physical processes that occur in the electrode sheath regions. In particular, there is uncertainty about the role of space-charge effects at the electrodes. For arcs with thermionic cathodes such as thoriated tungsten, Delalondre and Simonin (1990) and Zhu *et al.* (1992) have made analyses of the unified arc-cathode region and obtained reasonable agreement with experimental results, but omitted any consideration of space-charge effects. On the other hand, Zhou and Heberlein (1994) and Benilov and Marotta (1995) have also made analyses for thermionic cathodes, but have concluded that there is a space-charge sheath region which is central to arc-cathode behaviour and have obtained sheath voltages of 12 V or more for this region. For arcs with non-thermionic cathodes there is agreement that an important space-charge region exists, but there is uncertainty as to whether electrons are emitted by field emission from the cathode, or whether electrons are mainly produced by ionisation in the space-charge region. In the present paper it is suggested that a further mechanism may be dominant in producing electrons near the cathode, namely, the photoionisation of neutral gas atoms by resonance radiation from the arc plasma. Near the anode, there is generally an increased positive electric field due to the constriction of the arc at the electrode (Cobine 1958; Boulos *et al.* 1994). However, some papers have presented calculations indicating that there is a thin region at the anode surface

\* Dedicated to Professor Robert W. Crompton on the occasion of his seventieth birthday.

in which the electric field is negative (Dinulescu and Pfender 1980; Morrow and Lowke 1993; Nemchinsky 1994).

These issues are important, not only for scientific reasons, but also to allow quantitative calculations of heating effects on the electrodes by the arc plasma. For example, in arc welding it is desirable to be able to calculate the degree of melting (Lancaster 1984). The magnitude of the voltage drops at the electrodes affects the energy deposited on the electrodes. In ‘Gas Metal Arc Welding’, the cathode is generally of mild steel and is thus a non-thermionic emitter. If the current at the cathode surface is carried by electron emission, there is a significant cooling effect of the cathode through the electrons overcoming the work function of the cathode. On the other hand, if the current at the cathode surface is carried by positive ions, there is a major heating effect on the cathode from the deposition of energy through the neutralisation of the positive ions.

The space-charge analyses of Zhou and Heberlein (1994) and Benilov and Marotta (1995), for thermionic cathodes, were made assuming that the space-charge region is collisionless and of a thickness equal to the mean free path of the electrons. There are uncertainties as to the boundary conditions of electron temperature and density on the plasma side of this space-charge region. In the present paper we investigate the role of space-charge regions for thermionic and non-thermionic cathodes and also for the anode, using electron transport coefficients in a continuum approach. Solutions have been obtained spanning the arc plasma, the region of neutral plasma where charge densities are perturbed by diffusion from their equilibrium plasma values, and the space-charge region, where densities of positive and negative charges are unequal. Temperature variations of the plasma are omitted. Questions arise as to the validity of the use of the transport coefficients if the space-charge regions are very thin and where there are large gradients in charge densities, electric fields and temperature. However, significant information is obtained about the gross features of space-charge effects at the electrodes. Our results support the validity of the use of the ambipolar diffusion approximation as used by Zhu *et al.* (1992) and Morrow and Lowke (1993) to treat the non-equilibrium regions near thermionic cathodes and at the anode.

## 2. Theory

We obtain the spatial variation of the electron and ion densities, and the electric field in the electrode sheaths by solving the particle conservation equations as well as Poisson’s equation. The problem is treated in one dimension, and only steady-state properties of the arc are considered.

The electron current density, including contributions due to drift and diffusion, is given by

$$j_e = -en_e\mu_e E - eD \frac{dn_e}{dz}, \quad (1)$$

where  $e$  is the electron charge,  $n_e$  is the electron number density,  $\mu_e$  is the electron mobility,  $E$  is the electric field, and  $D$  is the electron diffusion coefficient.

The ion current density is similarly given by

$$j_+ = en_+\mu_+E, \quad (2)$$

where  $n_+$  is the ion density and  $\mu_+$  is the ion mobility, taken to be a factor of 100 less than the electron mobility. Diffusion current for the ions is neglected since it is generally much smaller than the drift current.

The electron continuity equation is

$$\frac{dj_e}{dz} = eS - e\gamma n_+ n_e, \quad (3)$$

where  $S$  is a source function representing thermal ionisation and  $\gamma$  is the recombination coefficient, both of which are taken to be constant within the sheath and the plasma. The magnitude of  $S$  is set equal to  $\gamma n_{eq}^2$ , where  $n_{eq}$  is the equilibrium value of  $n_e$  for the plasma temperature. In our calculations we have determined  $S$  using  $n_{eq} = 1.4 \times 10^{17} \text{ cm}^{-3}$ , which is the equilibrium electron density for argon at 15 000 K at 1 bar.

There is a similar equation for the continuity of positive ions given by

$$\frac{dj_+}{dz} = eS - e\gamma n_+ n_e. \quad (4)$$

When equation (4) is subtracted from equation (3) and then integrated, we obtain the total current density  $j$ , given by

$$j = j_e - j_+. \quad (5)$$

In equation (3) we have omitted the term  $n_e \alpha W$  usually used to represent ionisation by the electric field;  $\alpha$  is the ionisation coefficient, dependent on the field, and  $W$  is the electron drift velocity. For electric fields which vary very rapidly with distance, such a term will be highly inaccurate. For example at the cathode surface where the electric field is very high, this term would give very large ionisation, but the true ionisation at the cathode surface will be almost zero, because electrons emitted from the surface have not gained sufficient energy from the field to ionise the gas. In Section 4, we add a term to equation (3) to give an approximate account of ionisation.

The space-charge effects are determined by Poisson's equation

$$\frac{dE}{dz} = \frac{e}{\epsilon_0} (n_+ - n_e), \quad (6)$$

where  $\epsilon_0 = 8.85 \times 10^{-12} \text{ C V}^{-1} \text{ m}^{-1}$  is the permittivity of free space. The electric field  $E$  is related to the electric potential  $V$  by

$$\frac{dV}{dz} = -E. \quad (7)$$

Setting all of the spatial derivatives to zero and solving the resulting simultaneous equations for a given value of  $j$  defines the equilibrium values of the variables,

that is the values in the plasma of  $n_e, n_+, j_e, j_+$  and  $E$ . The value of  $V$  can be arbitrarily set to zero at  $z = 0$ .

The equations (1)–(3) and (5)–(7) can be expressed as four coupled first-order differential equations

$$\frac{dn_e}{dz} = -\frac{1}{D} \left( \mu_e n_e E + \frac{1}{e} j_e \right), \quad (8)$$

$$\frac{dj_e}{dz} = eS + \frac{\gamma(j - j_e)n_e}{\mu_+ E}, \quad (9)$$

$$\frac{dE}{dz} = \frac{1}{\varepsilon_0} \left( \frac{j_e - j}{\mu_+ E} - en_e \right), \quad (10)$$

$$\frac{dV}{dz} = -E, \quad (11)$$

and two subsidiary equations

$$n_+ = \frac{j_e - j}{e\mu_+ E}, \quad (12)$$

$$j_+ = j_e - j. \quad (13)$$

These equations define the six basic variables  $j_e, j_+, n_e, n_+, E$  and  $V$  for a given value of  $j$ .

Numerical solutions of these equations are not easily obtained by conventional algorithms for solving differential equations. In the region close to and within the uniform plasma, where  $n_e \approx n_+$ , they become intolerably ‘stiff’ due to equation (10). Stiff equations are discussed, for example, by Oran and Boris (1987) and Curtiss and Hirschfelder (1952). By assuming that the ion and electron densities are approximately equal in this region, the problem of stiffness can be solved. We replace Poisson’s equations (6) and (10) with

$$n_e = n_+, \quad (14)$$

so the resulting coupled ordinary differential equations for this region are

$$\frac{dn_e}{dz} = \frac{1}{eD\mu_+} [\mu_e j - (\mu_e + \mu_+) j_e], \quad (15)$$

$$\frac{dj_e}{dz} = eS - e\gamma n_e^2, \quad (16)$$

$$\frac{dV}{dz} = \frac{j - j_e}{e\mu_+ n_e}, \quad (17)$$

with  $j_+$  given by equation (13). The value of  $E$  is defined by equation (12) with  $n_+ = n_e$ , i.e.

$$E = \frac{j_e - j}{e\mu_+n_e}. \quad (18)$$

Equations (15)–(17) are integrated using a ‘predictor corrector’ technique (Hamming 1959), starting from the plasma, with  $j_e$  set at the equilibrium value and  $n_e$  perturbed to be slightly below the equilibrium value. Stepping towards the electrode, a point is reached where the set of equations, which includes Poisson’s equation, ceases to be stiff. From this point equations (8)–(11) can now be integrated to complete the solution. Other solutions are possible if the integration is commenced in the plasma, but with the value of  $n_e$  perturbed slightly above the equilibrium value, or with  $j_e$  perturbed either positively or negatively and with  $n_e$  at the equilibrium value. However, for these three solutions, the values of  $n_e$  at either the cathode or the anode increase above the plasma value so that boundary conditions cannot be satisfied at the electrodes.

The point of changeover between the two sets of equations is determined by the value of  $(n_+ - n_e)$  calculated from Poisson’s equation (6). We evaluate  $\epsilon$  from

$$\epsilon \equiv \left| \frac{n_+ - n_e}{n_e} \right| = \frac{\epsilon_0}{en} \left| \frac{dE}{dz} \right|, \quad (19)$$

where  $n$  is the value of  $n_e$  (and  $n_+$ ) calculated from the approximate equations. We evaluate  $dE/dz$  by differentiating equation (18) to obtain

$$\frac{dE}{dz} = \frac{n_e dj_e/dz - (j_e - j) dn_e/dz}{e\mu_+n_e^2}, \quad (20)$$

and use equations (15) and (16) to evaluate  $dn_e/dz$  and  $dj_e/dz$ , respectively. We change to the use of equations (8)–(13), which includes Poisson’s equation, when  $\epsilon$  is above a specified value. The quantity  $\epsilon$  can be considered a measure of the relative error in  $n_e$  and  $n_+$  when ignoring Poisson’s equation, and it is found that problems of stiffness are avoided if the changeover to the equations (8)–(13) occurs when  $\epsilon$  increases to 0.0005 (0.05%). Such an error is small enough to justify the approximation  $n_e = n_+$  near the uniform plasma. Later changeovers at larger integration distances allowing errors of up to 1% do not change the character of the solutions.

### 3. Results

We have used a constant electron mobility,  $\mu_e = 5000 \text{ cm}^2 \text{ s}^{-1} \text{ V}^{-1}$ ;  $\mu_e = W/E = \sigma/en_{eq}$  where the electrical conductivity  $\sigma = 100 \text{ ohm}^{-1} \text{ cm}^{-1}$  and  $n_{eq} = 1.4 \times 10^{-17} \text{ cm}^{-3}$  are approximate values at 15 000 K for the electrode sheaths (Murphy and Arundell 1994). The value of  $\mu_e$  is about a factor of 10 lower than the values of  $\mu_e$  at low  $E/N$  from Huxley and Crompton (1974) due to the influence of Coulomb collisions of electrons with ions. Ion mobility  $\mu_+$  is taken simply as  $\mu_e/100 = 50 \text{ cm}^2 \text{ s}^{-1} \text{ V}^{-1}$ . The largest uncertainty in the calculations is the value chosen for the recombination coefficient  $\gamma$ , which is a function of temperature. Only theoretical values exist for the high plasma temperatures of the order of 20 000 K. The value of  $\gamma$  also defines the value of the source term  $S$  from

$S = \gamma n_{eq}^2$ . In a preliminary account of this work (Lowke and Quartel 1995), a value of  $\gamma = 8.0 \times 10^{-10} \text{ cm}^3 \text{ s}^{-1}$  was chosen to coincide with the sheath calculations using the ambipolar diffusion of Morrow and Lowke (1993) and Zhu *et al.* (1992) so that comparisons could be made. In the present paper, we give solutions for  $\gamma = 10^{-11} \text{ cm}^3 \text{ s}^{-1}$ , at 15 000 K, this being more representative of both the value of  $10^{-12} \text{ cm}^3 \text{ s}^{-1}$  from the theoretical work of Biberman *et al.* (1973), and the value of  $10^{-10} \text{ cm}^3 \text{ s}^{-1}$  from the classical formula  $\gamma = 1.1 \times 10^{-8} n_e T^{-4.5} \text{ cm}^3 \text{ s}^{-1}$  of Hinnov and Hirschberg (1962), discussed by Mitchner and Kruger (1973). The electron diffusion coefficient  $D$  was calculated from  $kT\mu_e/e$ , using a plasma temperature of 15 000 K;  $k$  is Boltzmann's constant. Then  $D = 5900 \text{ cm}^2 \text{ s}^{-1}$  and using  $n_{eq} = 1.4 \times 10^{17} \text{ cm}^{-3}$ , we have  $S = 1.96 \times 10^{23} \text{ cm}^3 \text{ s}^{-1}$ .

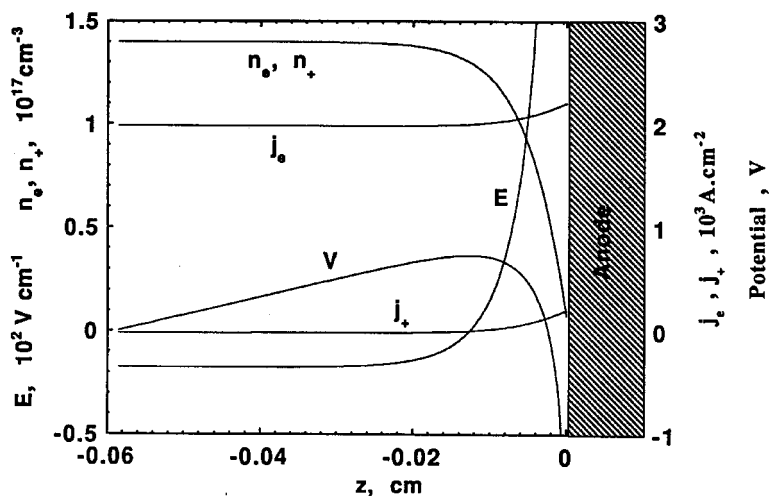


Fig. 1. Calculated electron and ion densities, electron and ion currents, electric field, and potential in the anode sheath, for an arc with current density  $j = 2000 \text{ A cm}^{-2}$  and with  $\gamma = 10^{-11} \text{ cm}^3 \text{ s}^{-1}$ .

The solution for the anode is shown in Fig. 1, with the anode boundary taken to be the point where the electron density falls to zero. The change in direction of the electric field is notable, and is due to the rapidly falling particle densities producing a large diffusion current. This diffusion current is greater than the drift current in the arc column and must therefore be offset by a negative drift current at the anode, requiring a retarding electric field. Fig. 2, an enlargement of the density curves closest to the anode, shows that space-charge plays a minor role. The distance over which  $n_e$  and  $n_+$  differ by more than 10% is of the order of the electron mean free path and the voltage drop over this space-charge sheath is about 0.2 V. It is seen from Fig. 1 that the anode voltage drop is negative, and for this calculation is about 2 V. The current density for this calculation of  $j = 2000 \text{ A cm}^{-2}$  is chosen to be at about the value found for a 200 A free burning arc with a plane anode (Zhu *et al.* 1992). Of course the present calculations do not take account of temperature variations. The cooler plasma near the anode will lead to a reduced electrical conductivity and will make a positive contribution to the anode fall.

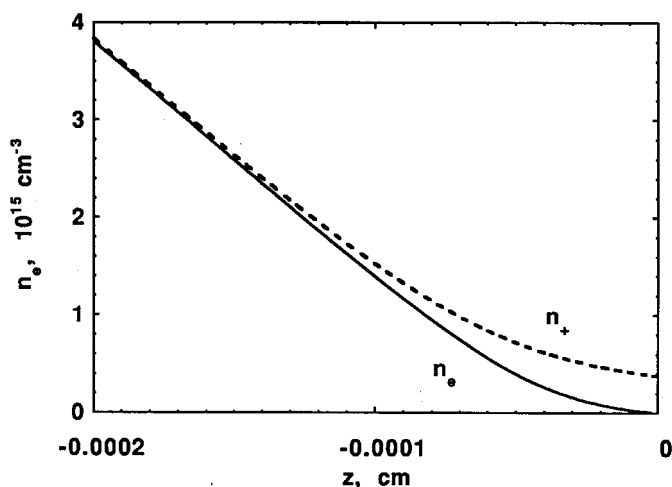


Fig. 2. Enlargement of the density solutions of Fig. 1 in the region close to the anode. Note the small charge separation.

The current density  $j = 28\,000\text{ A cm}^{-2}$ , for the cathode solution, shown in Fig. 3, is similarly chosen to be about the current density found at the cathode of a 200 A free burning arc (Zhu *et al.* 1992). The solution includes cases where the cathode is a thermionic emitter and also cases where emission is by secondary emission, the only difference being the position in Fig. 3 that is taken to be the cathode boundary. If the cathode emits thermionic current, then the boundary would be at the point where the value of  $j_e$  corresponds to the thermionic current. For this range of the solution of Fig. 3,  $n_e$  is approximately equal to  $n_+$  and the ambipolar approximation is thus valid.

For non-thermionic cathodes,  $j_e$  at the electrode surface is generally much less than  $j$ . Then the position of the cathode is further from the equilibrium plasma, with Fig. 3 showing the limiting position where  $j_e = 0$ . At the cathode surface there will be secondary emission of electrons due to the impinging positive ions. Thus the position of the cathode is determined by the value of  $z$  for which  $|j_e| = \Gamma|j_+|$ , where  $\Gamma$  is the secondary emission coefficient of the surface for the emission of electrons by positive ions. Values of  $\Gamma$  are typically  $\sim 0.1$  or less. However, even with  $\Gamma$  as high as 0.2, the cathode-fall voltage from Fig. 3 is of the order of megavolts and quite unrealistic.

In Fig. 4 we show an enlargement of the plot of electron and ion densities near the cathode of Fig. 3. We notice that there is a large region of charge separation near the electrode surface, where ion densities are several orders of magnitude larger than electron densities. The discrepancy between the calculated and observed potential difference between the plasma and the cathode, for non-thermionic materials, is very large. For example, experimental values of the total arc voltage with a cathode of iron are only about 20 V, whereas our solution, even with a value of  $\Gamma$  of 0.2, shows a potential at the cathode of several kilovolts for the earlier solution of Lowke and Quartel (1995) and megavolts for the present solution. Furthermore, at the position where the electric field is of the order of  $3 \times 10^7\text{ Vcm}^{-1}$  which is necessary for field emission (Dolan and Dyke



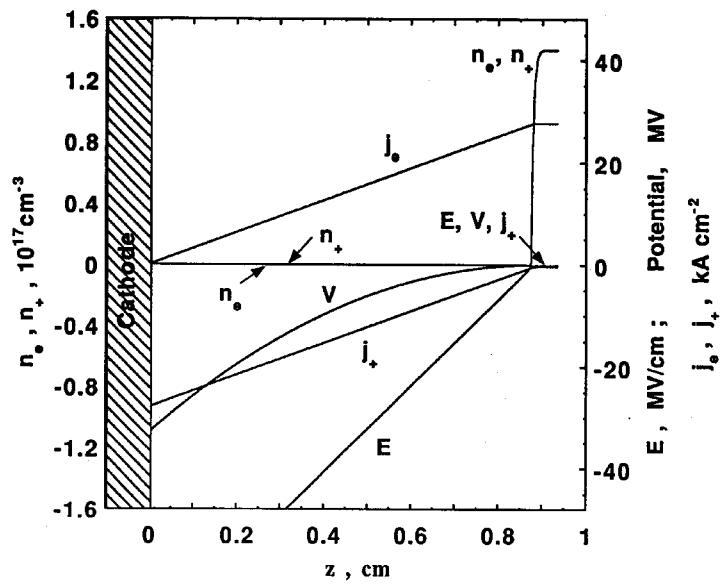


Fig. 3. Calculated electron and ion densities, electron and ion currents, electric field, and potential in the cathode sheath, for an arc with current density  $j = 28\,000 \text{ A cm}^{-2}$  and with  $\gamma = 10^{-11} \text{ cm}^3 \text{ s}^{-1}$ . Ionisation due to the electric field is not included.

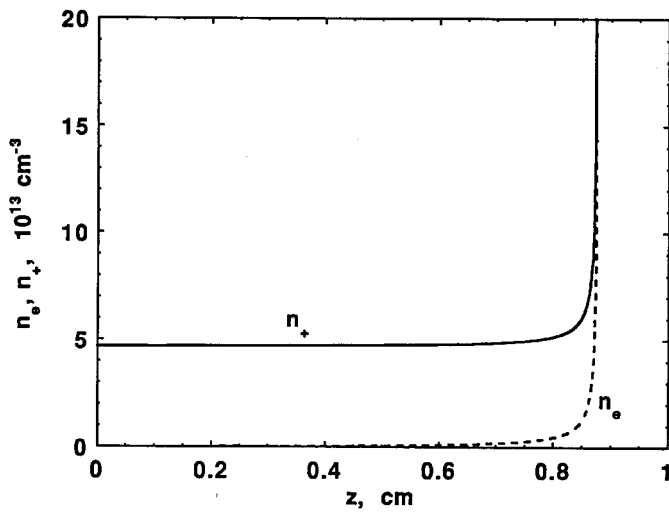


Fig. 4. Enlargement of the density solutions of Fig. 3 in the region close to the cathode.

1954), the potential of the cathode sheath is many orders of magnitude larger than observed arc voltages.

#### 4. Discussion

##### (4a) Ionisation in the Cathode Sheath

The unrealistically high voltages, calculated for non-thermionic cathodes, suggest that there is a source of electrons in the cathode region other than electrons from field emission. There are several possibilities. One is that the electrons are produced from ionisation by high energy ions accelerated within the sheath. But the ionisation cross sections for ions have a threshold approximately double that for electrons (Phelps 1991), so that this process is unlikely to be as significant as ionisation by electrons for the small arc voltages of the order of 20 V that are obtained using non-thermionic cathodes.

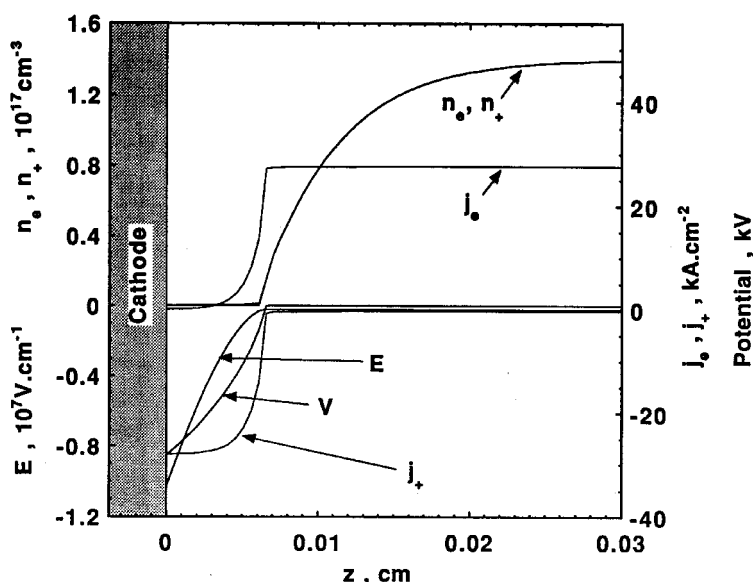


Fig. 5. Calculated quantities of Fig. 3, but with inclusion of ionisation due to the electric field using ionisation coefficients.

We now consider the possibility that the dominant source of electrons is ionisation by electrons accelerated by the electric field in the cathode sheath. In Fig. 5 we show calculations as for Fig. 3, but including the term  $n_e \alpha W$  in equation (3). Values of  $\alpha/N$  as a function of  $E/N$  were taken from Dutton (1975). It is seen from a comparison of Figs 3 and 5 that inclusion of the ionisation term reduces the thickness of the ionisation sheath to about 0.1 mm. However, the magnitude of the sheath voltage is still extremely high, being about 30 kV compared to the voltages of tens of megavolts shown in Fig. 3.

To model electron ionisation in a more realistic way than using equilibrium ionisation coefficients, an extra term in  $j_e$  was added to equation (3) to give

$$\frac{dj_e}{dz} = eS - e\gamma n_+ n_e - \frac{j_e [E - E(0)] \ln 2}{V_i}; \quad (21)$$

$E(0)$  is the electric field in the uniform plasma and  $V_i$  is the ionisation potential. This form is chosen because, neglecting the first two terms on the right of equation (21), integration gives an electron current proportional to  $2^{V/V_i}$ , where  $V = -\int E dz$ . Hence, moving from the cathode towards the uniform plasma, the electron current is doubled whenever the potential increases by an amount  $V_i$ .

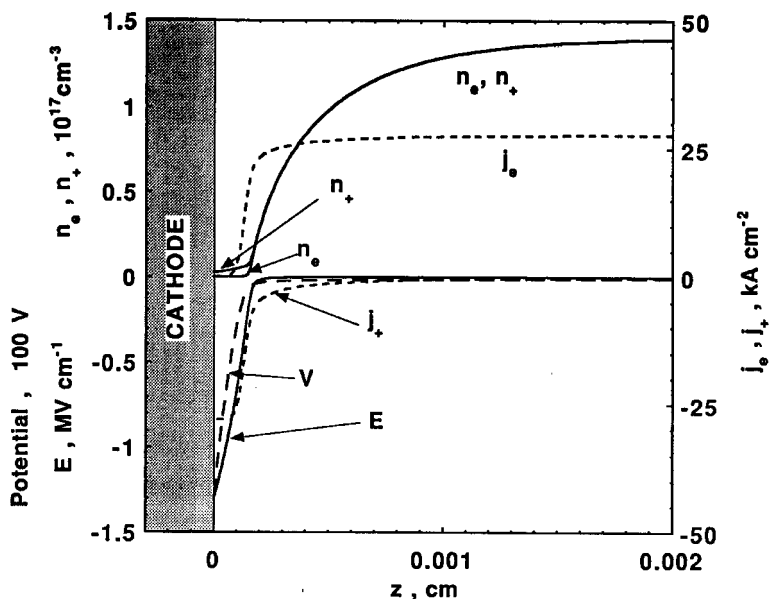


Fig. 6. Calculated quantities of Fig. 3, using a model for electron ionisation within the sheath, as in equation (21).

Fig. 6 shows the cathode solution using this revised model, with  $V_i = 7.9$  V appropriate for iron vapour, but with  $\gamma$  set at the low value of  $10^{-11}$   $\text{cm}^3 \text{s}^{-1}$ . The ionisation term dramatically increases the growth of the cathode current, resulting in a cathode fall voltage of about 100 V, which is orders of magnitude smaller than for Figs 3 and 5. Mechanisms such as two-step ionisation would reduce still further the predicted voltage. Observed sheath voltages of the order of 15 V for non-thermionic cathodes (Kesaev 1965) are still rather low, compared with the calculated voltages of Fig. 6, particularly when it is considered that this calculation gives an absolute maximum of ionisation growth due to the electric field, assuming that there is a current doubling for every increase in the sheath voltage equal to the ionisation potential. It is noted from Figs 5, 6 and 7 that the electric field at the cathode is still below that necessary for field emission.

Another possibility is that ionisation within the cathode sheath region is enhanced by photoionisation by radiation from the arc or that we have understated the source term because of a low value of  $\gamma$ . We have inferred  $S$  from  $\gamma n_{eq}^2$ , with  $\gamma = 10^{-11}$   $\text{cm}^3 \text{s}^{-1}$ . But Chen (1969) predicts that  $\gamma$  can be as high as

$10^{-7} \text{ cm}^3 \text{ s}^{-1}$ . We find that on increasing  $\gamma$  and thus  $S$  by a factor of  $10^4$ , with  $\gamma = 10^{-7}$ , the resulting cathode potential, for a non-thermionic emitter, is only  $\sim 8 \text{ V}$ . This solution is shown in Fig. 7 and is a much more realistic solution than that of Figs 3 and 5.

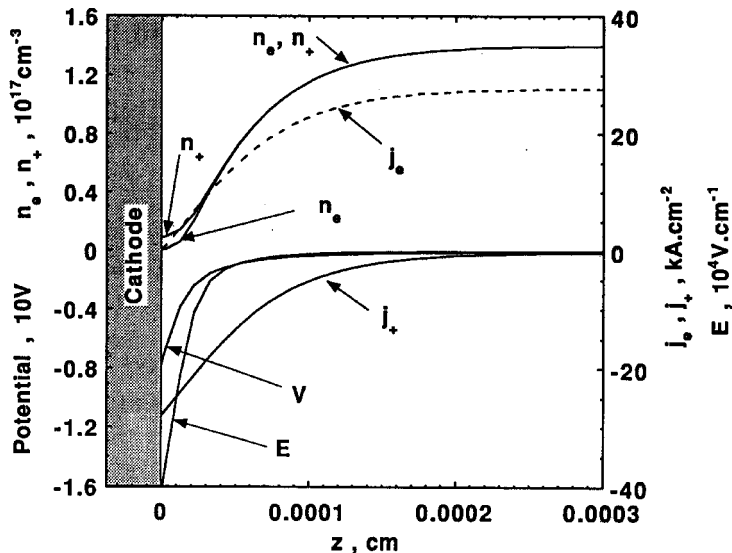


Fig. 7. Calculated quantities of Fig. 3 near the cathode with a current density of  $28\,000 \text{ A cm}^{-2}$  but with  $\gamma = 10^{-7} \text{ cm}^3 \text{ s}^{-1}$ . Ionisation due to the electric field is not included.

In all of our calculations, we have set the source term in the thin cathode sheath equal to the equilibrium plasma value of  $\gamma n_{eq}^2$ . However, this relationship does not always apply, for example, if electrons near the cathode are produced by photoionisation by resonance radiation from the arc plasma. Recent calculations have concluded that the radiation emission coefficient is increased by almost two orders of magnitude through the inclusion of the resonance lines in the far ultraviolet that are dominant at plasma temperatures of  $20\,000 \text{ K}$  (Boulos *et al.* 1994).

#### (4b) Effect of Ion Diffusion

The effect of ion diffusion could be included in the present calculations by adding a diffusion term  $-eD_+ dn_+/dz$  to equation (2) analogous to that in equation (1), where  $D_+$  is the ion diffusion coefficient. For the transformed equations in the 'stiff' portion of the solution, where  $n_e \approx n_+$ , the effect of this term is simply to produce an additional factor in the denominator of equation (15) so that  $D$  is multiplied by  $[1 + (D_+/\mu_+)/(D/\mu_e)]$ . If the electron and ion temperatures are equal, this factor is 2, using  $D/\mu_e = D_+/\mu_+ = kT/e$ . Thus the effect of including ion diffusion is to double the effect of diffusion, which is consistent with the formula for the ambipolar diffusion coefficient, of  $D_a = (D/\mu_e + D_+/\mu_+)/(1/\mu_e + 1/\mu_+)$  (Llewellyn-Jones 1966). In this formula,  $D_a$  is doubled if  $D_+/\mu_+ = D/\mu_e$  instead of  $D_+$  being zero.

Results of Figs 1 and 2 for the anode and of Fig. 3 for thermionic cathodes, suggest that the ambipolar diffusion approximation should be valid, because  $n_e$  and  $n_+$  are almost equal. However, a close examination of the results of Fig. 3 indicates that significant voltages develop as soon as the ion current is more than a few percent of the total current. If the ambipolar diffusion approximation is valid, calculations for the sheath regions can be made, accounting for temperature variations, but neglecting space-charge effects, as has been done by Delalondre and Simonin (1990) and by Zhu *et al.* (1992).

#### (4c) Analytic Formulae for Sheath Properties

It is useful to derive approximate analytic formulae for the thickness of the sheath regions. For the cathode space-charge region we assume that the electron density is zero, and define  $z = 0$  at the cathode boundary, where  $j = -j^+$ . If  $b$  is the space-charge sheath thickness, at  $z = b$ ,  $E$  and  $j_+$  are approximately zero. Integration of equation (4) gives

$$j_+ = eS(z - b), \quad (22)$$

so that the sheath thickness is given by

$$b = j/eS = j/e\gamma n_{eq}^2. \quad (23)$$

Using equations (2), (4) and (22) we obtain

$$E \frac{dE}{dz} = \frac{eS}{\varepsilon_0\mu_+}(z - b). \quad (24)$$

Integrating this equation and using the assumption that  $E \approx 0$  at  $x = b$  to eliminate the constant of integration, we obtain the following formulae:

$$E = \sqrt{eS/\varepsilon_0\mu_+}(z - b) = (e\gamma/\varepsilon_0\mu_+)^{\frac{1}{2}} n_{eq}(z - b), \quad (25)$$

$$n_+ = j_+/e\mu_+E = (\varepsilon_0S/e\mu_+)^{\frac{1}{2}} = (\varepsilon_0\gamma/e\mu_+)^{\frac{1}{2}} n_{eq}. \quad (26)$$

Similar formulae to the above were derived by Lowke and Davies (1977) in a different application. The numerical solutions agree well with this analysis. Cathode sheath thicknesses predicted by equation (23) are 0.89 cm and  $0.9 \times 10^{-4}$  cm, for Figs 3 and 7, respectively.

An approximate formula can also be derived for the thickness  $\Delta z$  of the region dominated by ambipolar diffusion; for example, at the anode. Then  $j_e$  is approximately given by  $-eD_a dn_e/dz$ , where  $D_a$  is the ambipolar diffusion coefficient. From equation (3), the gradient of  $j_e$  will be of the same order as  $e\gamma n_e^2$ . We make an approximation

$$\left| eD_a \frac{d^2 n_e}{dz^2} \right| = e\gamma n_e^2. \quad (27)$$

Further approximating  $|d^2n_e/dz^2|$  to be  $n_e/\Delta z^2$ , and using  $D_a/\mu = kT/e$ , we obtain

$$\Delta z = \sqrt{D_a/\gamma n_{eq}} = \sqrt{\frac{(kT/e)\mu_+}{\gamma n_{eq}}}. \quad (28)$$

Equation (28) gives a value  $\Delta z = 0.01$  cm for the diffusion-sheath thickness for  $\gamma = 10^{-11} \text{ cm}^3 \text{ s}^{-1}$ ,  $\mu_+ = 50 \text{ cm}^2 \text{ s}^{-1} \text{ V}^{-1}$ ,  $n_{eq} = 10^{17} \text{ cm}^{-3}$  and  $kT/e = 1$ , which compares well with the calculations of Figs 1 and 3, and  $\Delta z = 0.0001$  cm for  $\gamma = 10^{-7} \text{ cm}^3 \text{ s}^{-1}$ , which compares well with the calculation of Fig. 7.

## 5. Conclusion

Solutions to the equations of electron and ion continuity, and Poisson's equation, are calculated for the sheath regions of electric arcs. Even though no account is taken of temperature variations near the electrodes, useful conclusions can be made:

(1) For the anode region, the space-charge region is insignificant, and the ambipolar diffusion approximation should be valid.

(2) Gradients in charge density at the anode are so large that the diffusion current to the anode can be larger than the current in the column. Then a negative electrode voltage with respect to the plasma is necessary to provide a counter balancing negative drift current.

(3) For thermionic cathodes, the ambipolar-diffusion approximation should be valid, but significant voltages develop for ion currents of more than a few percent.

(4) For non-thermionic cathodes such as iron, the results suggest that field emission from the cathode is unlikely. Rather, the electron current is likely to be produced by ionisation in the cathode sheath. It is suggested that photoionisation by resonance radiation from the arc plasma, rather than ionisation from the electric field, could be a dominant effect.

## Acknowledgments

We are indebted to Dick Morrow and Tony Farmer, of our laboratories, for suggestions and discussions throughout this work. This project was supported in part by the Cooperative Research Centre for Materials Welding and Joining. We are also grateful for the contributions of Robert Winn, at an early stage of this project.

## References

- Benilov, M. S., and Marotta, A. (1995). *J. Phys. D* **28**, 1869–82.
- Biberman, L. M., Vorob'ev, V. S., and Yakubov, I. T. (1973). *Sov. Phys. Uspekhi* **15**, 375–531.
- Boulos, M. I., Fauchais, P., and Pfender, E. (1994). 'Thermal Plasmas: Fundamentals and Applications' (Plenum: New York).
- Chen, C. J. (1969). *J. Chem. Phys.* **50**, 1560–6.
- Cobine, J. (1958). 'Gaseous Conductors' (Dover: New York).
- Curtiss, C. F., and Hirschfelder, J. O. (1952). *Proc. Nat. Acad. Sci. USA* **38**, 235
- Delalandre, C., and Simonin, O. (1990). *Coll de Physique* **51**, C5, 199–206.
- Dinulescu, H. A., and Pfender, E. (1980). *J. Appl. Phys.* **51**, 3149–57.
- Dolan, W. W., and Dyke, W. P. (1954). *Phys. Rev.* **95**, 327–32.
- Dutton, J. (1975). *J. Phys. Chem. Ref. Data.* **4**, 577–713.
- Hamming, R. W. (1959). *J. Assoc. Comput. Mach.* **6**, 37.

- Hinnov, E., and Hirschberg, J. G. (1962). *Phys. Rev.* **125**, 795.
- Huxley, L. G. H., and Crompton, R. W. (1974). 'The Diffusion and Drift of Electrons in Gases' (Wiley: New York).
- Kesaev, I. G. (1965). *Sov. Phys. Technical Phys.* **9**, 1146–54.
- Lancaster, J. F. (1984). 'The Physics of Welding' (Pergamon: Oxford).
- Llewellyn-Jones, F. (1966). 'The Glow Discharge' (Methuen: London).
- Lowke, J. J., and Davies, D. K. (1977). *J. Appl. Phys.* **48**, 4991–5000.
- Lowke, J. J., and Quartel, J. C. (1995). Proc. Eleventh Int. Conf. on Gas Discharges and Their Applications, Tokyo, Vol. 1, pp. 90–3.
- Mitchner, M., and Kruger, C. H., Jr (1973). 'Partially Ionised Gases' (Wiley: New York).
- Morrow, R., and Lowke, J. J. (1993). *J. Phys. D* **26**, 634–42.
- Murphy, A. B., and Arundell, C. J. (1994). *Plasma Chem. Plasma Process* **14**, 451–90.
- Nemchinsky, V. A. (1994). *J. Phys. D* **27**, 2515–21.
- Oran, E. S., and Boris, J. P. (1987). 'Numerical Simulation of Reactive Flow' (Elsevier: New York).
- Phelps, A. V. (1991). *J. Phys. Chem. Ref. Data* **20**, 557.
- Zhou, X., and Heberlein, J. (1994). *Plasma Sources Sci. Technol.* **3**, 564–74.
- Zhu, P., Lowke, J. J., and Morrow, R. (1992). *J. Phys. D* **25**, 1221–30.